

Article

Tetra-, Penta- and Hexa-Coordinated Transition Metal Complexes Constructed from Coumarin-Containing N₂O₂ Ligand

Lei Gao, Chang Liu, Fei Wang and Wen-Kui Dong * 

School of Chemical and Biological Engineering, Lanzhou Jiaotong University, Lanzhou 730070, China; GaoLei19910731@163.com (L.G.); liuchang973914143@126.com (C.L.); wangfei3986@163.com (F.W.)

* Correspondence: dongwk@126.com; Tel.: +86-93-1493-8703

Received: 10 January 2018; Accepted: 30 January 2018; Published: 1 February 2018

Abstract: Three newly designed complexes, [Cu(L)]·CHCl₃ (**1**), [Co(L)(MeOH)]·CHCl₃ (**2**) and [{Ni(L)(MeOH)(PhCOO)}₂Ni] (**3**) a coumarin-containing Salamo-type chelating ligand (H₂L) have been synthesized and characterized by elemental analyses, IR and UV-VIS spectra, and X-ray crystallography. Complex **1** includes one Cu(II) atom, one completely deprotonated (L)²⁻ unit and one crystalline chloroform molecule, the Cu(II) atom shows a square-planar geometry. Complex **2** includes one Co(II) atom, one completely deprotonated (L)²⁻ unit, one coordinated methanol molecule and one crystalline chloroform molecule. The Co(II) atom is a distorted trigonal-bipyramidal geometry. While complex **3** includes three Ni(II) atoms, two completely deprotonated (L)²⁻ units, two benzoates and two coordinated methanol molecules. The complexes **1** and **2** are both possess three-dimensional supra-molecular structures by abundant noncovalent interactions. But, complex **3** formed a two-dimensional supra-molecular structure by intra-molecular hydrogen bonds. In addition, the antimicrobial and fluorescence properties of H₂L and its complexes **1**, **2** and **3** were also investigated.

Keywords: coumarin-containing N₂O₂ ligand; complex; synthesis; crystal structure; property

1. Introduction

Salen compound is a kind of versatile tetradentate N₂O₂ chelating ligand in modern coordination chemistry [1–7], and its metal complexes have been diffusely investigated in biological fields [8–10], ion recognitions [11], luminescent [12–17] and magnetic [18–21] materials, supra-molecular buildings [22–26] and so on. Especially, some substitution of atoms of the ligand with other elements often evidently improves its properties. When an *O*-alkyl oxime unit substitutes the imine moiety, the larger electronegativity of the O atoms is predicted to improve significantly the electronic behaviors of Salamo-type compounds, which may give rise to novel structures and better properties of the metal(II) complexes [27–33].

The introduction of different substituted groups into Salamo-type compounds may give rise to novel structures and the uncoordinated crystalline molecule can also affect the spatial structures [34–36]. Although these Salamo-type complexes have been in the process of development, the fluorescence and antimicrobial properties with coumarin-containing transition metal complexes are still unreported. In this study, three newly designed complexes [Cu(L)]·CHCl₃ (**1**), [Co(L)(MeOH)]·CHCl₃ (**2**) and [{NiL(MeOH)(PhCOO)}₂Ni] (**3**) have been prepared with a coumarin-containing Salamo-type N₂O₂ ligand, in particular the research on the Salamo-type complex contained benzoate ligands is reported firstly.

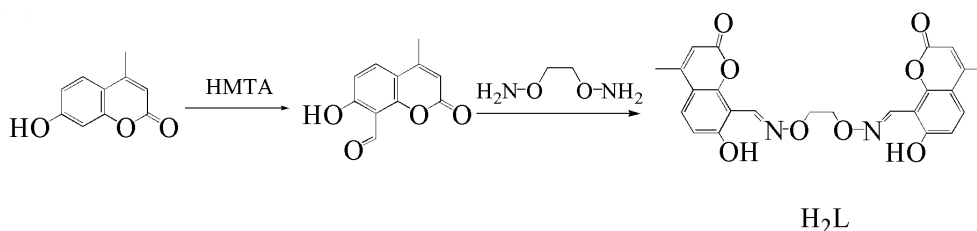
2. Experimental

2.1. Materials and Methods

7-Hydroxyl-4-methyl-coumarin (98%) was obtained from Alfa Aesar (New York, NY, USA). C, H and N analyses were gained by a GmbH VarioEL V3.00 automatic elemental analysis instrument (Elementar, Berlin, Germany). Elemental analyses for metals were obtained using an IRIS ER/S-WP-ICP atomic emission spectrometer (Elementar, Berlin, Germany). Melting points were measured by the use of a microscopic melting point apparatus made by Beijing Taike Instrument Limited Company (Beijing, China) and were uncorrected. IR spectra were recorded on a Vertex70 FT-IR spectrophotometer, with samples prepared as KBr (400–4000 cm^{-1}) pellets (Bruker AVANCE, Billerica, MA, USA). UV-VIS absorption spectra were measured on a Shimadzu UV-3900 spectrometer (Shimadzu, Tokyo, Japan). Luminescence spectra in solution were recorded on a Hitachi F-7000 spectrometer (Shimadzu, Tokyo, Japan). $^1\text{H-NMR}$ spectra were measured by a German Bruker AVANCE DRX-400 spectrometer (Bruker AVANCE, Billerica, MA, USA). X-ray single-crystal structures were determined by a SuperNova Dual (Cu at zero) and Bruker APEX-II CCD diffractometers (Bruker AVANCE, Billerica, MA, USA), respectively.

2.2. Synthesis of H_2L

Major reaction step, *O,O'*-ethane-1,2-diyl-bis-hydroxylamine was prepared following the literature [37–39]. 7-Hydroxy-4-methyl-2-oxo-2*H*-chromene-8-carbonitrile was synthesized in accordance with the reported procedures [40]. The major reaction steps participated in the preparation of H_2L are shown in Scheme 1.



Scheme 1. Synthetic route to H_2L .

An ethanol solution (15 mL) of 7-Hydroxy-4-methyl-2-oxo-2*H*-chromene-8-carbonitrile (384.38 mg, 1.45 mmol) was added dropwise to an ethanol solution (15 mL) of *O,O'*-ethane-1,2-diyl-bis-hydroxylamine (46.00 mg, 0.5 mmol) in ethanol (15 mL) and the mixture was subjected to heating at 65–70 $^{\circ}\text{C}$ for 3 h. After cooling to the room temperature, the resulting white solid was collected. Yield, 186.47 mg, 0.40 mmol (80.3%). Anal. Calcd for $\text{C}_{24}\text{H}_{20}\text{N}_2\text{O}_8$ (%): C, 62.07; H, 4.34; N, 6.03; Found: C, 62.25; H, 4.47; N, 5.89. $^1\text{H-NMR}$ (400 MHz, CDCl_3), δ 10.72 (s, 2H, OH), 8.95 (s, 2H, CH=N), 7.50 (d, $J = 8.9$ Hz, 2H, ArH), 6.93 (d, $J = 8.9$ Hz, 2H, ArH), 6.14 (s, 2H, ArH), 4.54 (s, 4H, CH_2), 2.40 (s, 6H, CH_3).

2.3. Synthesis of Complex 1

A chloroform solution (4 mL) of H_2L (4.64 mg, 0.01 mmol) was added dropwise to a methanol solution (4 mL) of $\text{Cu}(\text{OAc})_2 \cdot \text{H}_2\text{O}$ (1.99 mg, 0.01 mmol), the color of the mixed solution changes immediately to dark green. The mixed solution was filtered, and the filtrate was kept undisturbed in the dark to avoid decomposition of the coumarin-containing building blocks. Single-crystals suitable for X-ray crystallography were grown up by partial solvent evaporation after about two weeks, and collected carefully by filtration, washed with *n*-hexane, and dried at room temperature. Yield, 3.01 mg, 0.0047 mmol (46.7%). Anal. Calc. for $\text{C}_{25}\text{H}_{19}\text{Cl}_3\text{CuN}_2\text{O}_8$ (%): C, 46.53; H, 2.97; N, 4.34; Cu, 9.85; Found: C, 46.69; H, 3.02; N, 4.17; Cu, 9.71.

2.4. Synthesis of Complex 2

A solution of H₂L (4.64 mg, 0.01 mmol) in 4 mL of chloroform was added dropwise to a methanol solution (6 mL) of Co(NO₃)₂·6H₂O (2.91 mg, 0.01 mmol). The color of the mixed solution changes immediately to brown. The mixed solution was filtered, and the filtrate kept undisturbed in the dark to avoid decomposition of the coumarin-containing building blocks. Single-crystals suitable for X-ray crystallography were grown up by partial solvent evaporation after about one week, and collected carefully by filtration, washed with n-hexane, and dried at room temperature. Yield, 3.32 mg, 0.0049 mmol (49.3 %). Anal. Calc. for C₂₆H₂₃Cl₃CoN₂O₉ (%): C, 46.42; H, 3.45; N, 4.16; Co, 8.76; Found: C, 46.61; H, 3.57; N, 4.02; Co, 8.61.

2.5. Synthesis of Complex 3

A chloroform solution (4 mL) of H₂L (4.64 mg, 0.01 mmol) was added dropwise to a methanol solution (2 mL) of Ni(NO₃)₂·6H₂O (2.90 mg, 0.01 mmol). Then, a methanol solution (5 mL) of sodium benzoic (1.22 mg, 0.01 mmol) was added, and the mixed solution was kept stirring for 5 min at room temperature. The mixed solution was filtered, and the filtrate kept undisturbed in the dark to avoid decomposition of the coumarin-containing building blocks. Single-crystals suitable for X-ray crystallography were grown up by partial solvent evaporation after about three weeks, and collected carefully by filtration, washed with n-hexane, and dried at room temperature. Yield, 2.05 mg, 0.0015 mmol (43.7%). Anal. Calc. for C₆₄H₅₄N₄Ni₃O₂₂ (%): C, 54.62; H, 3.87; N, 3.98; Ni, 12.51; Found: C, 54.81; H, 3.93; N, 3.83; Ni, 12.33.

2.6. X-ray Crystal Structure Determinations for Complexes 1, 2 and 3

X-ray single crystal diffraction data of the complexes **1**, **2** and **3** were recorded using a SuperNova Dual (Cu at zero) and Bruker APEX-II CCD diffractometers with a monochromated Mo-K α radiation ($\lambda = 0.71073 \text{ \AA}$) source at 296(2), 173.00(10) and 153(2) K, respectively. The LP corrections were applied to the SAINT program [41] and Semi-empirical correction were applied to the SADABS program [42]. The single crystal structures were solved by the direct methods (SHELXS-2014) [43]. All hydrogen atoms were added theoretically and difference-Fourier map exhibited the positions of the remaining atoms. The H atoms were included at the calculated positions and constrained to ride on their parent atoms. All non-hydrogen atoms were refined anisotropically by a full-matrix least-squares procedure on F^2 with SHELXL-2014 [43]. Crystal data and refinement parameters involved the structure determinations are presented in Table 1.

Table 1. Crystal data and refinement parameters for complexes **1**, **2** and **3**.

Complex	1	2	3
Formula	C ₂₅ H ₁₉ Cl ₃ CuN ₂ O ₈	C ₂₆ H ₂₃ Cl ₃ CoN ₂ O ₉	C ₆₄ H ₅₄ N ₄ Ni ₃ O ₂₂
Formula weight	645.31	672.74	1407.24
Temperature (K)	296(2)	173.00(10)	153(2)
Wavelength (Å)	0.71073	0.71073	0.71073
Crystal system	Monoclinic	Monoclinic	Triclinic
Space group	<i>P</i> 2 ₁ / <i>c</i>	<i>P</i> 2 ₁ / <i>c</i>	<i>P</i> -1
Unit cell dimensions			
<i>a</i> (Å)	13.5401(9)	12.1129(5)	12.6250(18)
<i>b</i> (Å)	6.8318(5)	13.5779(3)	12.6344(17)
<i>c</i> (Å)	27.1822(16)	16.7455(6)	14.7046(18)
α (°)	90	90	113.420(4)
β (°)	94.8504(19)	100.038(3)	95.978(5)
γ (°)	90	90	107.557(2)
<i>V</i> (Å ³)	2505.4(3)	2711.93(15)	1983.6(5)
<i>Z</i>	4	4	1
<i>D</i> _c (g cm ⁻³)	1.711	1.648	1.178
μ (mm ⁻¹)	1.247	0.987	0.770

Table 1. Cont.

Complex	1	2	3
<i>F</i> (000)	1308	1372	726
Crystal size (mm)	0.26 × 0.22 × 0.19	0.16 × 0.07 × 0.04	0.22 × 0.19 × 0.18
θ Range (°)	2.219–25.005	3.416–26.020	1.750–25.010
Index ranges	−16 ≤ <i>h</i> ≤ 16, −8 ≤ <i>k</i> ≤ 6 −32 ≤ <i>l</i> ≤ 31	−9 ≤ <i>h</i> ≤ 14, −16 ≤ <i>k</i> ≤ 15 −20 ≤ <i>l</i> ≤ 20	−13 ≤ <i>h</i> ≤ 15 −15 ≤ <i>k</i> ≤ 15 −17 ≤ <i>l</i> ≤ 16
Reflections collected	16385	10655	14781
Independent reflections	4402	5343	6919
<i>R</i> _{int}	0.0746	0.0410	0.0661
Completeness	99.9%	99.7%	99.0%
Data/restraints/parameters	4402/0/354	5343/4/376	6919/69/319
GOF	1.097	1.053	1.050
Final <i>R</i> ₁ , <i>wR</i> ₂ indices	0.0659, 0.1066	0.0585, 0.1315	0.0579, 0.1580
<i>R</i> ₁ , <i>wR</i> ₂ indices (all data)	0.1058, 0.1207	0.0861, 0.1530	0.0890, 0.1779
Largest differences	0.364/−0.439	1.211/−0.653	0.935/−0.828
	peak and hole (e Å ^{−3})		

Crystallographic data have been deposited with the Cambridge Crystallographic Data Centre as supplementary publication, No. CCDC 1,816,001, 1,816,000 and 1,816,002 for complexes **1**, **2** and **3**, respectively. Copies of the data can be gained free of charge on application to CCDC, 12 Union Road, Cambridge CB21EZ, UK (Telephone: (44) 01223 762910; Fax: +44-1223-336033; E-mail: deposit@ccdc.cam.ac.uk). These data can be also obtained free of charge at www.ccdc.cam.ac.uk/conts/retrieving.html.

3. Results and Discussion

Complexes **1**, **2** and **3** a coumarin-containing Salamo-type ligand have been prepared, and characterized by IR, UV-VIS and X-ray crystallography methods. In addition, the fluorescence properties of complexes **1**, **2** and **3** and antimicrobial activities of H₂L and its complexes **1**, **2** and **3** were also investigated.

3.1. IR Spectra

The FT-IR spectra of H₂L with its corresponding complexes **1**, **2** and **3** possess different bands in the 4000–400 cm^{−1} region (Figure 1 and Table 2).

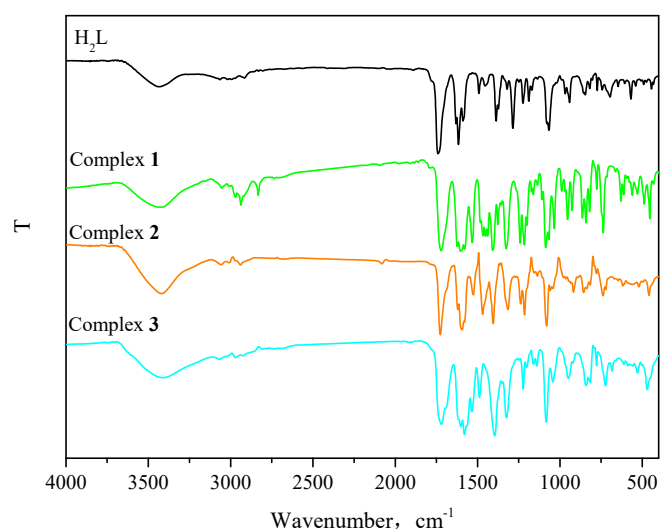


Figure 1. The FT-IR spectra of H₂L and its complexes **1**, **2** and **3** (cm^{−1}).

Table 2. The major FT-IR spectra of H₂L and its complexes **1**, **2** and **3** (cm⁻¹).

Compound	$\nu(\text{C=N})$	$\nu(\text{Ar-O})$	$\nu(\text{C=O})$	$\nu(\text{C=C})$
H ₂ L	1616	1282	1734	1386
Complex 1	1601	1242	1722	1320
Complex 2	1597	1238	1726	1312
Complex 3	1605	1222	1719	1325

The characteristic C=O stretching band at 1734 cm⁻¹ of the ligand H₂L, and those of the complexes **1**, **2** and **3** emerge at 1722, 1726 and 1719 cm⁻¹, respectively [44]. Meanwhile, a characteristic C=N stretching band of H₂L emerges at 1616 cm⁻¹, and those of complexes **1**, **2** and **3** show at 1601, 1597 and 1605 cm⁻¹, respectively [45]. The characteristic C=N stretching frequencies are moved to low frequencies, which indicates that the metal(II) atoms are bonded by azomethine N atoms of the ligand (L)²⁻ moieties [46]. H₂L presents a characteristic Ar-O stretching frequency at 1282 cm⁻¹, while those of complexes **1**, **2** and **3** emerge at 1242, 1238 and 1222 cm⁻¹, respectively. The characteristic Ar-O stretching frequencies are moved to low frequencies, which can be evidence for formation of Cu-O, Co-O and Ni-O bonds between Cu(II), Co(II) and Ni(II) atoms with O atoms of phenolic groups [47].

3.2. UV-VIS Spectra

The UV-VIS absorption spectra of H₂L with its complexes **1**, **2** and **3** in the dichloromethane solutions (2.0×10^{-5} M) at 298 K are shown in Figure 2 and Table 3. The absorption peaks of H₂L are different from its complexes **1**, **2** and **3**. The absorption spectrum of H₂L comprises three relatively intense absorption peaks centered at 291, 330 and 345 nm, the first peak at 291 nm can be assigned to the π - π^* transitions of the phenyl rings [48], the second peak at 330 nm can be assigned to the π - π^* transitions of the oxime group [49], and the third peak at 345 nm can be assigned to the n- π^* transitions of lactone carbonyl group [50]. Upon coordination of H₂L, the π - π^* transitions of the phenyl rings in complexes **1** and **2** are bathochromically shifted to 299 and 297 nm, respectively, and the absorption peak at 291 nm vanishes from the UV-VIS spectrum of complex **3**, indicating the coordination of Co(II), Cu(II) and Ni(II) atoms with the (L)²⁻ units [48]. Compared with H₂L, the absorption peak at 330 nm vanishes from the UV-VIS spectra of complexes **1**, **2** and **3**, indicating that the oxime N atoms are participated in coordination to the Cu(II), Co(II) and Ni(II) atoms [49]. Meanwhile, the n- π^* transitions of the lactone carbonyl group in complexes **1**, **2** and **3** assumes a hypsochromic shift to 343, 347 and 338 nm exhibiting that the coordination of the (L)²⁻ units with Cu(II), Co(II) and Ni(II) atoms, respectively. Meanwhile, three weak broad absorption peaks are gained at 396, 399 and 391 nm for complexes **1**, **2** and **3**, respectively, these new absorption peaks can be attributed to L→M charge-transfer transitions (LMCT). This is characteristic of N₂O₂-donors sphere with the transition metal complexes [49].

3.3. Fluorescence Properties

The fluorescent properties of H₂L and its complexes **1**, **2** and **3** were measured at room temperature (Figure 3). The ligand H₂L exhibits a strong and broad emission at 432 nm upon excitation at 351 nm, which should be assigned to intraligand π - π^* transition [12]. The complexes **1**, **2** and **3** display weakened photoluminescence with maximum emission peaks at ca. 417, 462 and 469 nm upon excitation at 351 nm, respectively. The absorption peaks are bathochromically-shifted of complexes **1** and **2**, and hypsochromically-shifted of complex **3**, which could be attributed to LMCT [12].

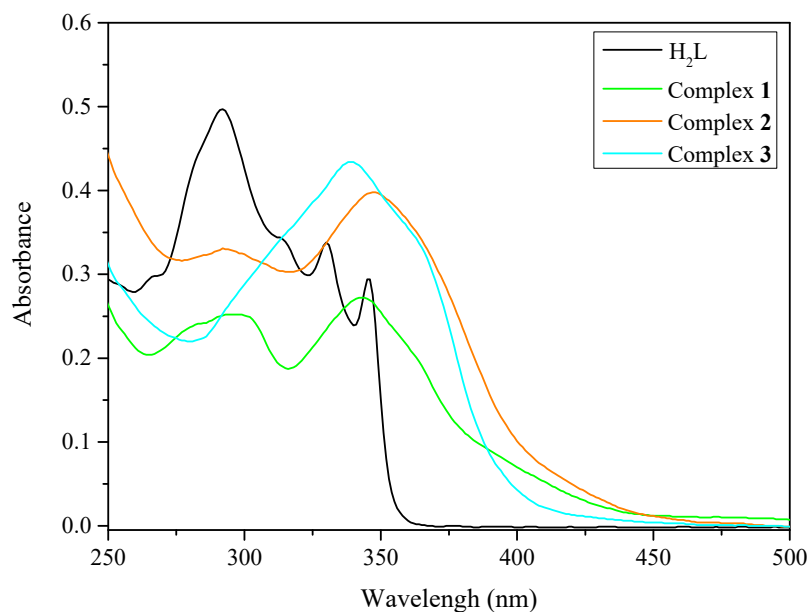


Figure 2. The UV-VIS spectra of H₂L and its complexes 1, 2 and 3 (cm⁻¹).

Table 3. Absorption maxima and molar extinction coefficients for H₂L and its complexes 1, 2 and 3.

Compound	λ_{max1} , nm	ϵ_{max1} , M ⁻¹ ·cm ⁻¹	λ_{max2} , nm	ϵ_{max2} , M ⁻¹ ·cm ⁻¹	λ_{max3} , nm	ϵ_{max3} , M ⁻¹ ·cm ⁻¹
H ₂ L	291	4.9×10^{-4}	330	3.3×10^{-4}	345	2.9×10^{-4}
Complex 1	299	2.5×10^{-4}	343	2.7×10^{-4}	396	0.7×10^{-4}
Complex 2	297	3.2×10^{-4}	347	3.9×10^{-4}	399	0.9×10^{-4}
Complex 3	338	4.3×10^{-4}	391	0.7×10^{-4}		

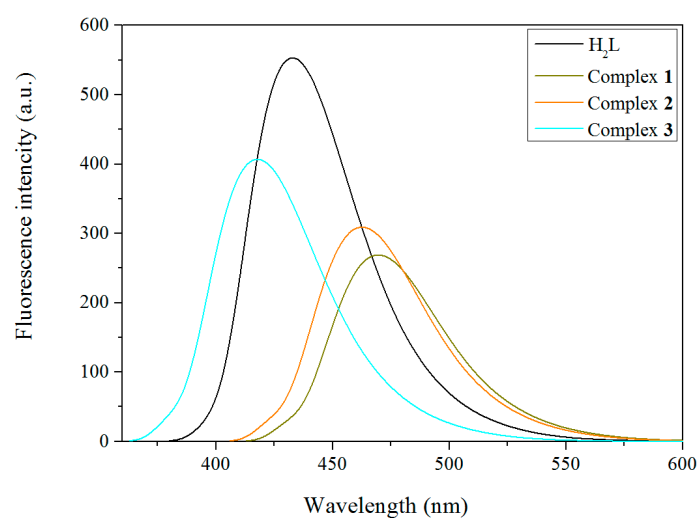


Figure 3. Emission spectra of H₂L and its complexes 1, 2 and 3 in dichloromethane (2.5×10^{-5} M) upon excitation at 351 nm.

3.4. Crystal Structure Description of Complex 1

As presented in Figure 4 and Table 4, complex 1 crystallizes in the monoclinic system, space group $P 2_1/c$, which comprises one Cu(II) atom, one deprotonated (L)²⁻ unit and one crystallizing chloroform molecule.

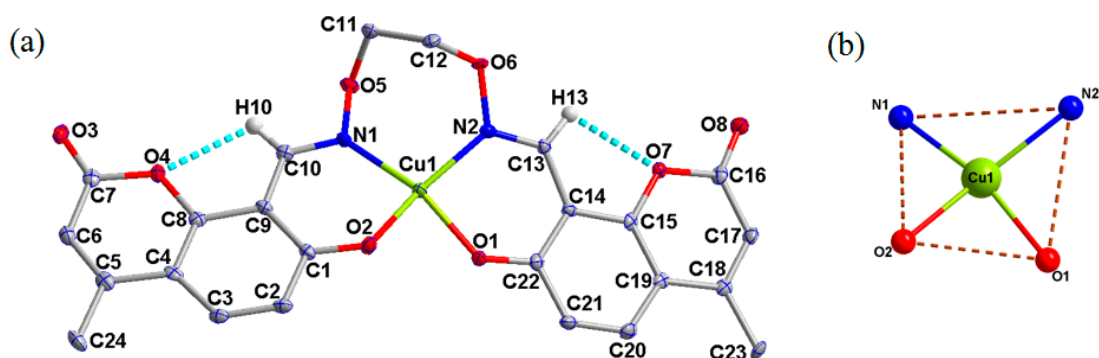


Figure 4. (a) X-ray crystal structure and atom numbering of complex **1** with 30% probability displacement ellipsoids; (b) Coordination polyhedron of Cu(II) atom of complex **1**.

Table 4. Selected bond lengths (Å) and angles (°) for complex **1**.

Bond			
Cu1-O1	1.891(3)	Cu1-N1	1.950(4)
Cu1-O2	1.909(3)	Cu1-N2	1.976(4)
Angles			
O1-Cu1-O2	83.86(14)	O1-Cu1-N2	90.30(15)
O1-Cu1-N1	162.19(18)	O2-Cu1-N2	161.44(17)
O2-Cu1-N1	89.28(15)	N1-Cu1-N2	100.99(16)

The Cu(II) atom is tetra-coordinated by two oxime N (N1 and N2) atoms and two deprotonated phenoxo O (O1 and O2) atoms, the four atoms are all from one deprotonated (L)²⁻ unit (Figure 4a). Geometry of Cu(II) atom can be best described as a slightly distorted square-planar with CuN_2O_2 coordination and deduced by using τ_4 index, $\tau_4 = 0.258$ (Figure 4b) [51]. The two phenolic O (O1 and O2) atoms and the two oxime N (N1 and N2) atoms of the (L)²⁻ unit compose together the basal ($Cu1-O1$, 1.891(3); $Cu1-O2$, 1.909(3); $Cu1-N1$, 1.950(4) and $Cu1-N2$, 1.976(4) Å) with N2 and O2 above average by 0.239(2) and 0.292(2) Å, and N1 and O1 below average by 0.241(2) and 0.289(2) Å, respectively. Additionally, dihedral angles between the basal planes (N_2O_2 plane) and the benzene rings are 13.17(2)° and 14.74(2)°, respectively, which defined as shown in Figure 5a. Dihedral angle of planes $N1-Cu1-N2$ and $O1-Cu1-O2$ is 22.37(2)° (Figure 5b) [52].

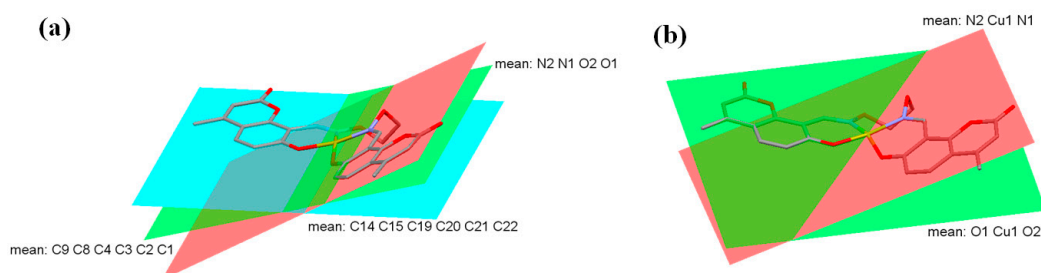


Figure 5. (a) View of the dihedral angles between the benzene rings and the N_2O_2 basal plane of complex **1**; (b) View of the dihedral angles between planes CuN_2 and CuO_2 of complex **1**.

As illustrated in Figure 6 and Table 5, complex **1** molecules form an infinite three-dimensional supra-molecular structure by inter-molecular hydrogen bonds, four pairs of inter-molecular hydrogen bonds $C12-H12B \cdots O1$, $C20-H20 \cdots O3$, $C25-H25 \cdots O8$ and $C12-H12A \cdots Cl1$ are formed [53].

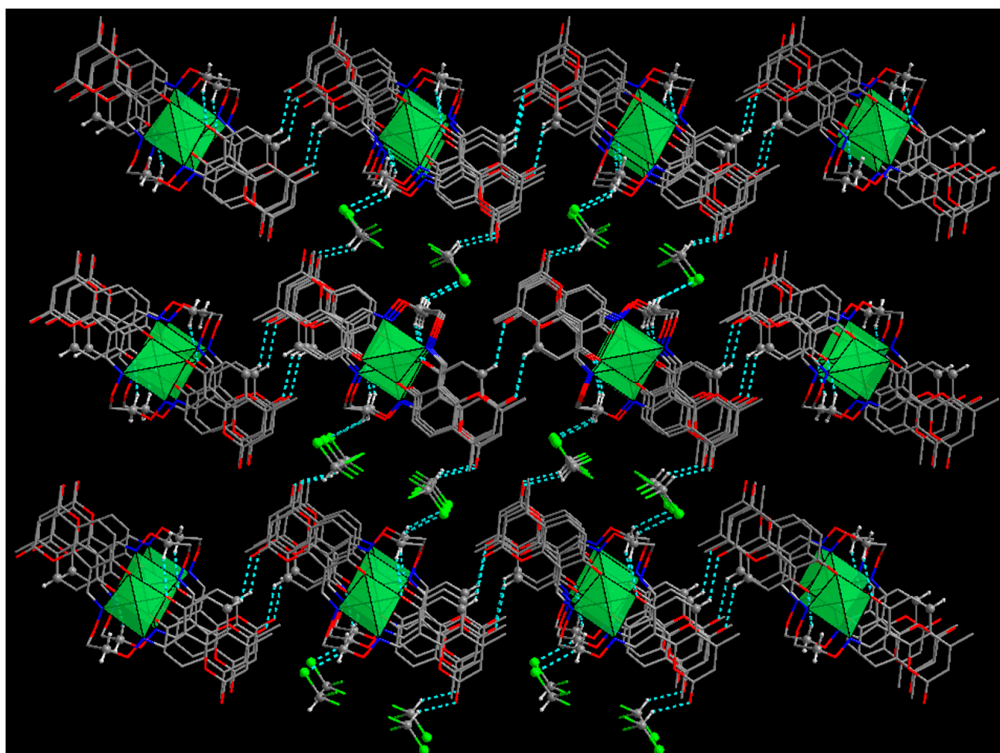


Figure 6. View of the three-dimensional supra-molecular structure of complex 1 showing the C-H...O, C-H...Cl hydrogen bondings.

Table 5. Hydrogen bondings (\AA , $^\circ$) for complex 1.

D-H · A	D · A	D-H · A
C10-H10 · O4	2.724(6)	103
C13-H13 · O7	2.715(5)	103
C12-H12B · O1	3.495(6)	156
C20-H20 · O3	3.284(6)	133
C25-H25 · O8	3.071(7)	141
C12-H12A · Cl1	3.561(6)	136

3.5. Crystal Structure Description of Complex 2

Complex 2 presents a symmetric mononuclear structure, crystallizes in the monoclinic system, space group $P 2_1/c$, composes one Co(II) atom, one deprotonated (L)²⁻ unit, one coordinated methanol molecule and one crystallizing chloroform molecule. Selected bond lengths and angles are listed in Table 6.

Table 6. Selected bond lengths (\AA) and angles ($^\circ$) for complex 2.

Bond			
Co1-O1	2.008(3)	Co1-N1	2.014(3)
Co1-O6	1.926(3)	Co1-N2	2.150(3)
Co1-O9	2.039(3)		
Angles			
O1-Co1-O9	90.67(12)	O6-Co1-N1	124.97(14)
O1-Co1-N1	88.52(12)	O6-Co1-N2	86.65(12)
O1-Co1-N2	178.25(13)	O9-Co1-N2	91.00(13)
O6-Co1-O1	93.23(11)	N1-Co1-O9	124.07(14)
O6-Co1-O9	110.91(13)	N1-Co1-N2	90.12(12)

As shown in Figure 7, the Co(II) atom is penta-coordinated by two oxime N (N1 and N2) and phenoxo O (O1 and O6) atoms from one deprotonated (L)²⁻ unit, and one O (O9) atom from the coordinated methanol molecule (Figure 7a). The coordination around the Co(II) atom is depicted as a trigonal bipyramid [54], and the τ value was estimated to be $\tau = 0.888$ (Figure 7b) [55]. The phenolic O (O6) atom and the oxime N (N1) atom of the (L)²⁻ unit and one O (O9) atom of the coordinated methanol molecule compose together the basal plane (Co1-O6, 1.926(3); Co1-N1, 2.014(3) and Co1-O9, 2.039(3) Å), and other phenolic O (O6) atom and oxime N (N1) atom of the (L)²⁻ unit hold the axial positions (Co1-O1, 2.008(3) and Co1-N2, 2.150(3) Å). The dihedral angles of the N₂O₂ basal plane and the benzene rings are 30.35(2)° and 33.16(2)°, respectively, which defined as shown in Figure 8a. The dihedral angle of the planes N1-Co1-N2 and O1-Co1-O2 is 55.11(2)° (Figure 8b) [56].

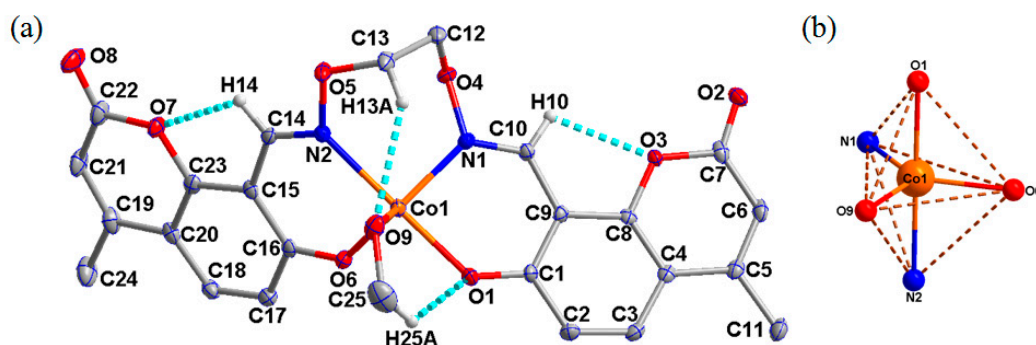


Figure 7. (a) X-ray crystal structure and atom numbering of complex 2 with 30% probability displacement ellipsoids; (b) Coordination polyhedron for Co(II) atom of complex 2.

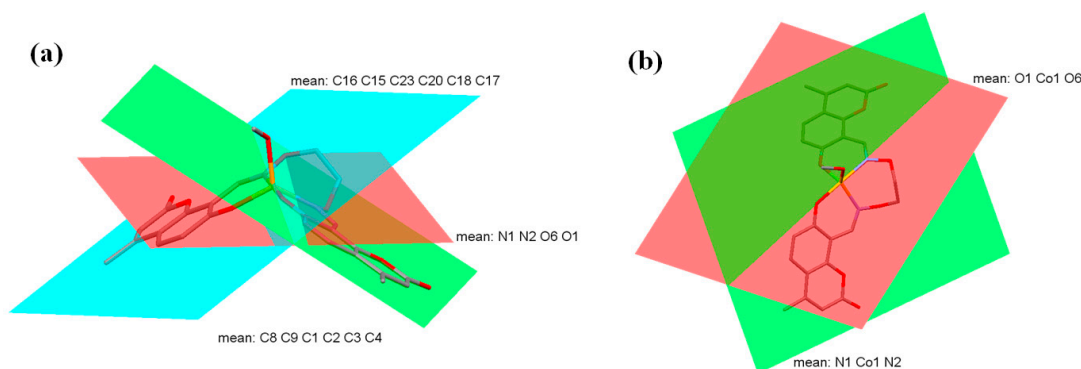


Figure 8. (a) View of the dihedral angles between the benzene rings and the N₂O₂ basal plane of complex 2; (b) View of the dihedral angles between the planes CoN₂ and CoO₂ of complex 2.

As shown in Figure 9 and Table 7, the three-dimensional supra-molecular network of complex 2 is made up of two parts. The first part is linked by inter-molecular hydrogen bond interactions, and five pairs of inter-molecular hydrogen bonds, C9-H9...O2, C6-H6...O6, C13-H13B...O2, C26-H26...O8 and C25-H25C...Cl3 are formed. The another part is made up of the C-Cl... π interactions. The Cg6 (C₁₅-C₁₆-C₁₇-C₁₈-C₂₀-C₂₃) of phenyl as acceptors forms two stacking interactions with the protons (-C26Cl1 and -C26Cl2). The Cg4 (O₇-C₁₉-C₂₃) of pyrone ring as acceptor forms one stacking interaction with -C26Cl2. In addition, complex 2 molecules form a three-dimensional infinite structure by O-H...O, C-H...O, C-H...Cl hydrogen bonds and C-Cl... π stacking interactions [57,58].

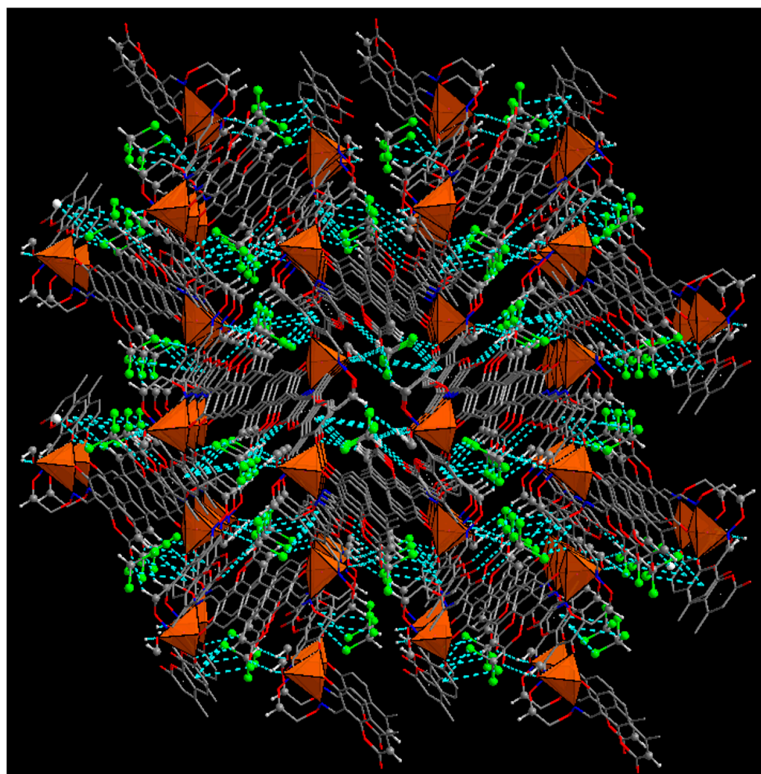


Figure 9. View of the three-dimensional supra-molecular structure of complex 2 exhibiting the C-H...O, O-H...O, C-H...Cl hydrogen bondings and C-Cl... π stacking interactions.

Table 7. Hydrogen bondings (\AA , $^\circ$) for complex 2.

D-H...A	D...A	D-H...A		
C10-H10...O3	2.682(4)	104		
C13-H13A...O9	3.433(6)	145		
C14-H14...O7	2.712(5)	103		
C25-H25A...O1	3.041(7)	125		
O9-H9...O2	2.651(4)	166		
C6-H6...O6	3.315(4)	139		
C13-H13B...O2	3.309(5)	134		
C26-H26...O8	3.146(6)	156		
C25-H25C...Cl3	3.642(6)	159		
D-X...A	D-X	X...A	D...A	D-X...A
C26-Cl1...Cg6	1.757(5)	3.824	4.415(5)	97.59
C26-Cl2...Cg6	1.757(5)	3.849	4.415(5)	96.78
C26-Cl2...Cg4	1.757(5)	3.655	4.557(5)	109.67

Note: Cg6 = C₁₅-C₁₆-C₁₇-C₁₈-C₂₀-C₂₃; Cg4 = O₇-C₁₉-C₂₃.

3.6. Crystal Structure Description of Complex 3

As illustrated in Figure 10 and Table 8, complex 3 exhibits a symmetric trinuclear structure, crystallizes in the triclinic system, space group $P\bar{1}$, includes two completely deprotonated (L)²⁻ units, three Ni(II) atoms, two benzoates and two coordinated methanol molecules.

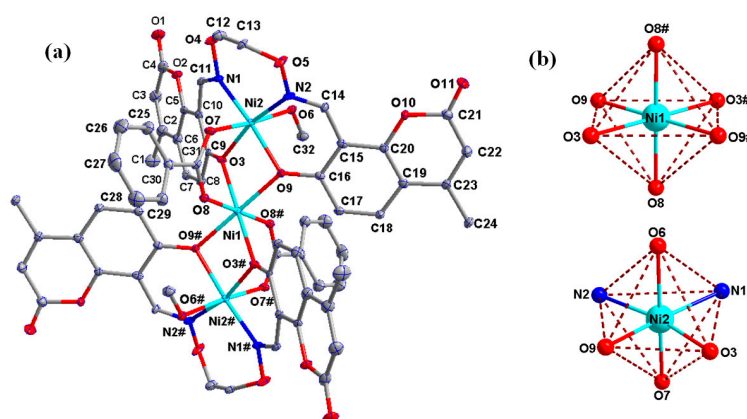


Figure 10. (a) X-ray crystal structure and atom numbering of complex **3** with 30% probability displacement ellipsoids; (b) Coordination polyhedrons for Ni(II) atoms of complex **3**.

Table 8. Selected bond lengths (Å) and angles (°) for complex **3**.

Bond			
Ni1-O3	2.082(3)	Ni2-O3	2.014(3)
Ni1-O3#	2.082(3)	Ni2-O6	2.150(3)
Ni1-O8	2.031(3)	Ni2-O7	2.018(3)
Ni1-O8#	2.031(3)	Ni2-O9	2.040(3)
Ni1-O9#	2.089(3)	Ni2-N1	2.068(4)
Ni1-O9	2.089(3)	Ni2-N2	2.069(4)
Angles			
O3-Ni1-O3#	180.0	O3-Ni2-O6	93.13(12)
O3#-Ni1-O9	101.51(11)	O3-Ni2-O9	80.97(11)
O3-Ni1-O9#	101.51(11)	O3-Ni2-N1	87.44(13)
O3-Ni1-O9	78.49(11)	O7-Ni2-O3	90.35(13)
O3#-Ni1-O9#	78.49(11)	O7-Ni2-O6	175.38(11)
O8#-Ni1-O3#	90.07(12)	O7-Ni2-O9	94.69(12)
O8#-Ni1-O3	89.93(12)	O7-Ni2-N1	91.74(15)
O8-Ni1-O3#	89.93(12)	O7-Ni2-N2	90.06(15)
O8-Ni1-O3	90.07(12)	O9-Ni2-O6	88.86(12)
O8#-Ni1-O8	180.0	O9-Ni2-N1	166.76(13)
O8#-Ni1-O9#	88.56(12)	O9-Ni2-N2	85.38(13)
O8-Ni1-O9	88.56(12)	N1-Ni2-O6	85.38(14)
O8#-Ni1-O9	91.44(12)	N1-Ni2-N2	106.20(14)
O8-Ni1-O9#	91.44(12)	N2-Ni2-O6	87.29(15)
O9#-Ni1-O9	180.0		

The terminal Ni2 atom is hexa-coordinated by two phenolic O (O3 and O9) and two oxime N (N1 and N2) atoms of the completely deprotonated (L)²⁻ moiety, one O (O7) atom from the coordinated benzoate group and one O (O6) atom from the coordinated methanol molecule. The terminal Ni2 atom possesses a distorted octahedron geometry [59]. The two oxime N (N1 and N2) and phenolic O (O3 and O9) atoms are in mutually *cis*-positions. Then, the central Ni1 atom is completed by double μ_2 -phenoxo O (O3 and O9) atoms from two (L)²⁻ moieties and two O (O8 and O8#) atoms from two benzoate groups. Each of the benzoate groups bridges the central Ni1 and terminal Ni2 atoms in the *syn-syn* bridging mode, as a result the central Ni1 atom finally possesses an O₂O₂O₂ coordination environment (Figure 10b) [59]. The dihedral angles between the benzene rings of (L)²⁻ moieties and the N₂O₂ basal plane are 32.87(2)° and 23.66(2)°, respectively, which defined as shown in Figure 11a. The dihedral angle between the planes of N1–Ni2–N2 and O3–Ni2–O9 is 6.50(2)° (Figure 11b) [59].

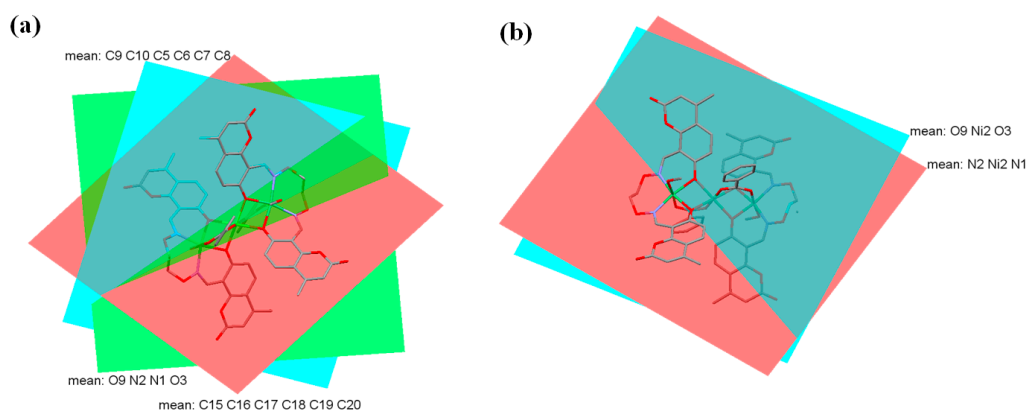


Figure 11. (a) View of the dihedral angles between the benzene rings and the N_2O_2 basal plane of complex 3; (b) View of the dihedral angles between the planes NiN_2 and NiO_2 of complex 3.

As depicted in Figure 12 and Table 9, in complex 3, seven pairs of intra-molecular hydrogen bonds $C8-H8 \cdots O8$, $C8-H8 \cdots O9$, $C11-H11 \cdots O2$, $C12-H12B \cdots N2$, $C13-H13B \cdots O7$, $C14-H14 \cdots O10$ and $C32-H32C \cdots O8$ are formed [60,61]. The protons ($-C11H11$) and ($-C14H14$) of $(L)^{2-}$ moieties form hydrogen bondings with two ester O ($O2$ and $O10$) atoms of $(L)^{2-}$ moieties, respectively. The proton ($-C12H12B$) from ethylenedioxiime carbon atom of $(L)^{2-}$ moieties forms hydrogen bonding with oxime N ($N2$) atom. The proton ($-C13H13B$) from ethylenedioxiime carbon atom of the $(L)^{2-}$ moiety forms hydrogen bonding with carboxylate O ($O7$) atom of coordinated benzoate group. The proton ($-C32H32C$) from coordinated methanol molecule form hydrogen bonding with O ($O8$) atom of coordinated benzoate group. The proton ($-C8H8$) of the $(L)^{2-}$ moiety forms hydrogen bonds with phenoxo O ($O9$) atom of $(L)^{2-}$ moiety and carboxylate O ($O8$) atom of coordinated benzoate group, respectively [62,63].

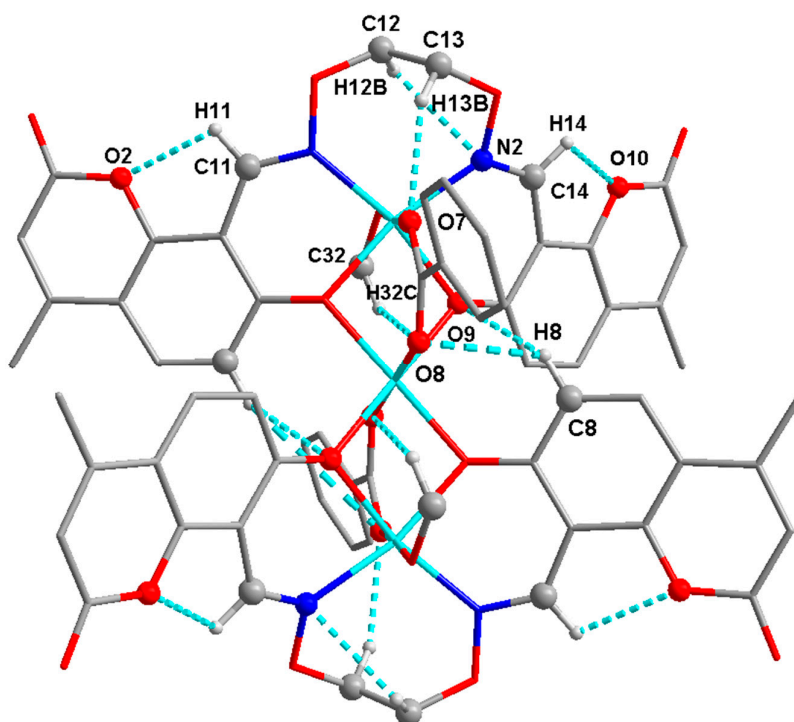


Figure 12. Intra-molecular $C-H \cdots O$ and $C-H \cdots N$ hydrogen bonds of complex 3.

Table 9. Hydrogen bondings (Å, °) for complex 3.

D-H...A	D...A	D-H...A
C8-H8...O8	3.176(6)	122
C8-H8...O9	3.289(5)	133
C11-H11...O2	2.661(6)	103
C12-H12B...N2	2.878(9)	102
C13-H13B...O7	3.110(8)	142
C14-H14...O10	2.673(6)	101
C32-H32C...O8	3.362(6)	155
O6-H6...O1	2.741(5)	164
C12-H12A...O11	3.180(8)	154

As illustrated in Figure 13, two pairs of inter-molecular hydrogen bondings, O6-H6...O1 and C12-H12A...O11 are formed. The proton (-C12H12A) of the $(L)^{2-}$ moiety forms hydrogen bondings with the O (O11) atom of four adjacent complex 3 molecules. Meanwhile, the proton (-O6H6) of the coordinated methanol molecule forms hydrogen bondings with the O (O1) atom from the $(L)^{2-}$ moiety of four adjacent complex 3 molecules. The space skeleton of complex 3 possesses a two-dimensional supra-molecular structure by the hydrogen bonding interactions [64].

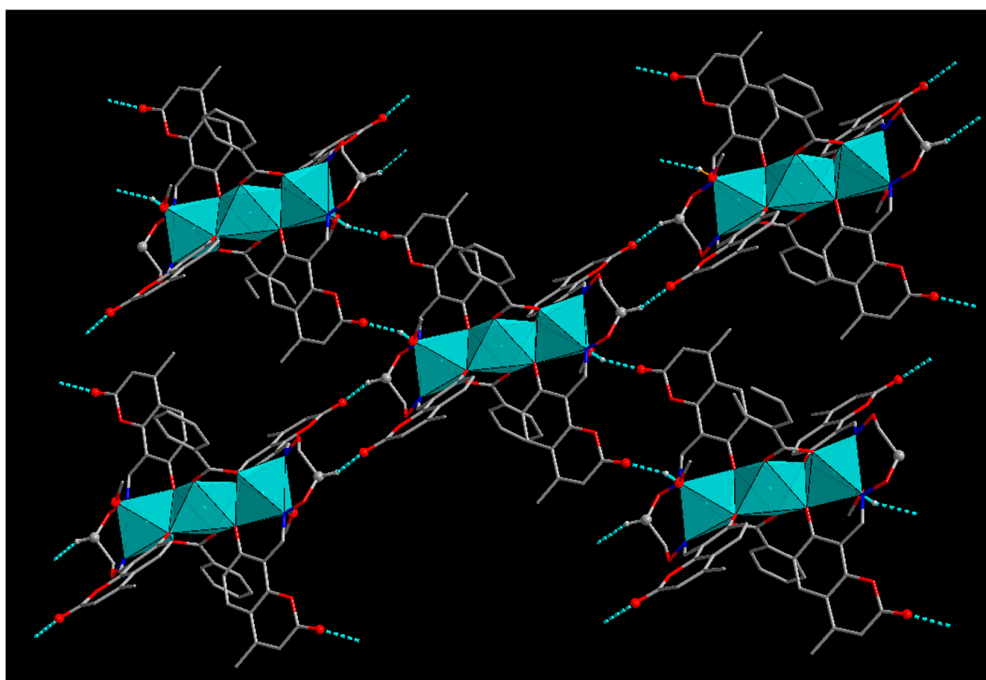


Figure 13. View of the two-dimensional supra-molecular structure of complex 3 exhibiting the O-H...O, C-H...O hydrogen bonding interactions.

Complexes 1, 2 and 3 with a coumarin-containing Salamo-type ligand H_2L have been synthesized, and have different structures depending on the anions and cations used. In complexes 1, 2 and 3, the metal atom located at the Salamo N_2O_2 unit is tetra-, penta- and hexa-coordinated, respectively. As widely known, the coordination number of Cu(II) atom is generally four or five in Salamo-type Cu(II) complexes and the coordination geometry around Cu(II) atom is planar quadrilateral, tetrahedron or tetragonal pyramid [26,37,49,51]. In complex 1, the coordination number of Cu(II) atom is four, the anions and the solvent molecules were not involved in the coordination. The coordination number of Co(II) atom is generally six, and the coordination geometry around Co(II) atom is octahedron [47,56,63,65]. While in complex 2, the methanol molecule was involved in the coordination

forming a mono-nuclear Co(II) complex. The coordination geometry around Co(II) atom is trigonal bipyramid, which is rare in the previously reported Salamo-type Co(II) complexes. In complex 3, both of the anions and the solvent molecules were involved in the coordination, this coordination pattern is frequently appeared in the Salamo-type trinuclear Ni(II) complexes, in which the three Ni(II) atoms are all hexa-coordinated with slightly distorted octahedral geometries [12,31,44,59], but the research on the Salamo-type trinuclear Ni(II) complex contained benzoate ligands is reported firstly.

3.7. Antimicrobial Activities

Bacteriostasis tests on common bacteria, such as *E. coli* and *S. aureus*, were carried out by the punch method. A small amount (0.1 mL) of a fresh overnight bacterial suspension was added into autoclaved LB (lysogeny broth) agar, then the agar was poured into sterile dishes. The concentration of the test compounds were 0.6, 1.2 and 2.4 mg/mL. 70 μ L of samples were added into a burrowed hole measuring 5 mm in diameter with transfer liquid gun when the medium underwent solidification [65,66].

As shown in Figures 14 and 15, the zones of DMF, metal salts, H₂L and complexes 1, 2 and 3 have apparent differences in antibacterial activity among two kinds of bacteria. The complexes 1, 2 and 3 displayed more enhanced antimicrobial activities than H₂L under the same conditions (2.5 mg/mL), and the DMF and the metal salts also have a weak biological activity. Moreover, *E. coli* shows stronger antibacterial activity, whereas *S. aureus* possesses weaker antibacterial activity. This increase in the antibacterial activities of complexes 1, 2 and 3 were accompanied with an increase in concentration and can be explained on the basis of the chelation theory [65,66]. Chelation reduces the polarity of the metal atom mainly due to partial share of positive charge of metal atom with donor groups and possible delocalization of π -electron within the whole chelate ring. Further, it enhances the lipophilic character of the central atom [66].

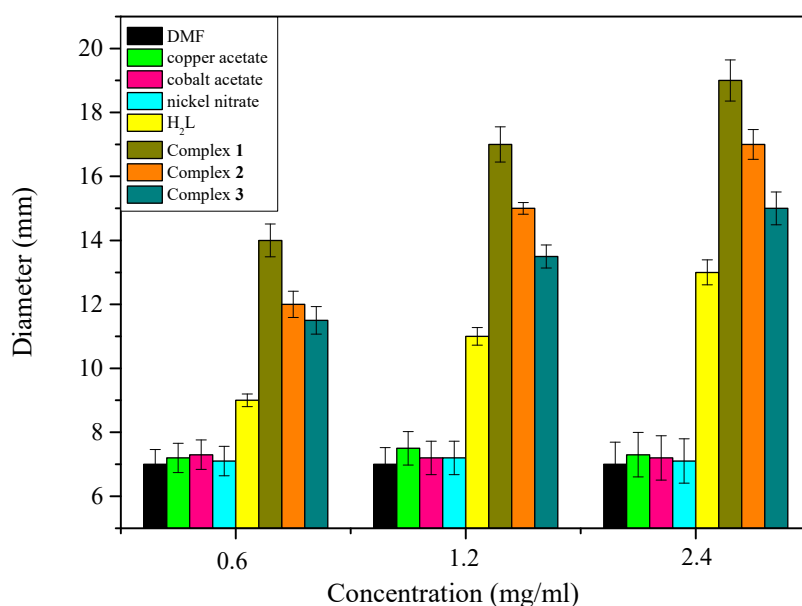


Figure 14. The diameter of inhibition zones of *E. coli* in different concentrations.

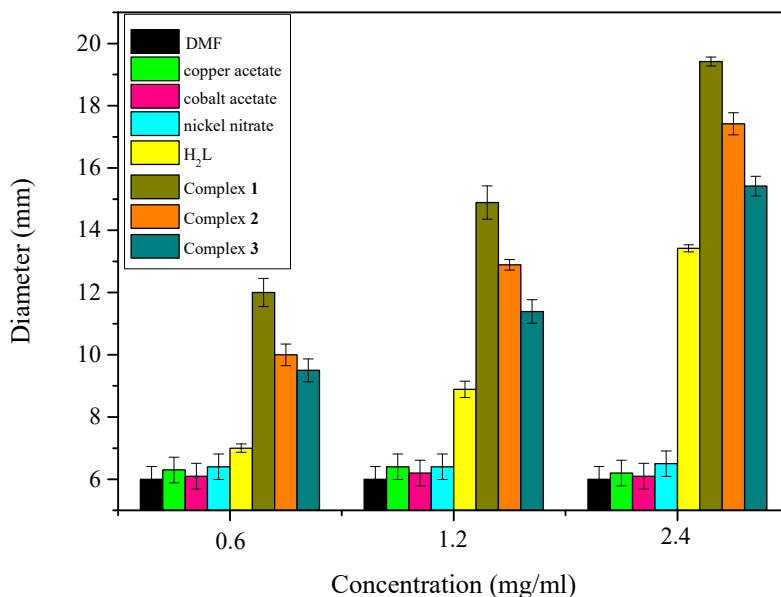


Figure 15. The diameter of inhibition zones of *S. aureus* in different concentrations.

4. Conclusions

In summary, three newly designed complexes $[\text{Cu}(\text{L})]\cdot\text{CHCl}_3$ (**1**), $[\text{Co}(\text{L})(\text{MeOH})]\cdot\text{CHCl}_3$ (**2**) and $[\{\text{Ni}(\text{L})(\text{MeOH})(\text{PhCOO})\}_2\text{Ni}]$ (**3**) derived from a Salamo-type coumarin-containing ligand (H_2L) have been successfully prepared and well characterized. For the central metals, the Cu(II) atom of complex **1** is tetra-coordinated and the Co(II) atom of complex **2** is penta-coordinated with trigonal-bipyramidal geometry, and the Ni(II) atoms of complex **3** are hexa-coordinated possessing slightly distorted octahedral geometries. The complexes **1** and **2** are both possess the three-dimensional supra-molecular structures by abundant noncovalent interactions. But complex **3** is formed a two-dimensional supra-molecular structure by intra-molecular hydrogen bonds. Furthermore, the antimicrobial and fluorescence properties of H_2L and complexes **1**, **2** and **3** were also studied.

Acknowledgments: This work was supported by the National Natural Science Foundation of China (21761018) and the Program for Excellent Team of Scientific Research in Lanzhou Jiaotong University (201706), which is gratefully acknowledged.

Author Contributions: W.-K.D. supervised the project and contributed materials/reagents/analysis tools; C.L. and F.W. performed the experiments; W.-K.D., L.G. wrote the manuscript.

Conflicts of Interest: The authors declare no conflict of interest.

References

1. Zhao, L.; Dang, X.T.; Chen, Q.; Zhao, J.X.; Wang, L. Synthesis, crystal structure and spectral properties of a 2D supramolecular copper(II) complex with 1-(4-[(*E*)-3-ethoxyl-2-hydroxybenzylidene]amino)phenyl)ethanone oxime. *Synth. React. Inorg. Met.-Org. Nano-Met. Chem.* **2013**, *43*, 1241–1246. [[CrossRef](#)]
2. Wu, H.L.; Pan, G.L.; Bai, Y.C.; Wang, H.; Kong, J.; Shi, F.; Zhang, Y.H.; Wang, X.L. Preparation, structure, DNA-binding properties, and antioxidant activities of a homodinuclear erbium(III) complex with a pentadentate Schiff base ligand. *J. Chem. Res.* **2014**, *38*, 211–217. [[CrossRef](#)]
3. Sun, Y.X.; Zhang, S.T.; Ren, Z.L.; Dong, X.Y.; Wang, L. Synthesis, characterization, and crystal structure of a new supramolecular Cd^{II} complex with halogen-substituted salen-type bisoxime. *Synth. React. Inorg. Met.-Org. Nano-Met. Chem.* **2013**, *43*, 995–1000. [[CrossRef](#)]
4. Song, X.Q.; Liu, P.P.; Liu, Y.A.; Zhou, J.J.; Wang, X.L. Two dodecanuclear heterometallic $[\text{Zn}_6\text{Ln}_6]$ clusters constructed by a multidentate salicylamide salen-like ligand: Synthesis, structure, luminescence and magnetic properties. *Dalton Trans.* **2016**, *45*, 8154–8163. [[CrossRef](#)] [[PubMed](#)]

5. Xu, L.; Zhu, L.C.; Ma, J.C.; Zhang, Y.; Zhang, J.; Dong, W.K. Syntheses, structures and spectral properties of mononuclear Cu^{II} and dimeric Zn^{II} complexes an asymmetric Salamo-type N₂O₂ ligand. *Zeitschrift für Anorganische und Allgemeine Chemie* **2015**, *641*, 2520–2524. [[CrossRef](#)]
6. Wang, P.; Zhao, L. Synthesis and crystal structure of supramolecular copper(II) complex N₂O₂ coordination Sphere. *Asian J. Chem.* **2015**, *4*, 1424–1426. [[CrossRef](#)]
7. Sun, Y.X.; Wang, L.; Dong, X.Y.; Ren, Z.L.; Meng, W.S. Synthesis, characterization, and crystal structure of a supramolecular Co^{II} complex containing Salen-type bisoxime. *Synth. React. Inorg. Met-Org. Nano-Met. Chem.* **2013**, *43*, 599–603. [[CrossRef](#)]
8. Wu, H.L.; Bai, Y.C.; Zhang, Y.H.; Pan, G.L.; Kong, J.; Shi, F.; Wang, X.L. Two lanthanide(III) complexes the schiff base *N,N*-Bis(salicylidene)-1,5-diamino-3-oxapentane: Synthesis, characterization, DNA-binding properties, and antioxidation. *Zeitschrift für Anorganische und Allgemeine Chemie* **2014**, *640*, 2062–2071. [[CrossRef](#)]
9. Wu, H.L.; Bai, Y.; Yuan, J.K.; Wang, H.; Pan, G.L.; Fan, X.Y.; Kong, J. A zinc(II) complex with tris(2-(*N*-methyl)benzimidazolymethyl)amine and salicylate: Synthesis, crystal structure, and DNA-binding. *J. Coord. Chem.* **2012**, *65*, 2839–2851. [[CrossRef](#)]
10. Chen, C.Y.; Zhang, J.W.; Zhang, Y.H.; Yang, Z.H.; Wu, H.L. Gadolinium(III) and dysprosium(III) complexes with a Schiff base bis(*N*-salicylidene)-3-oxapentane-1,5-diamine: Synthesis, characterization, antioxidation, and DNA-binding studies. *J. Coord. Chem.* **2015**, *68*, 1054–1071. [[CrossRef](#)]
11. Wang, F.; Gao, L.; Zhao, Q.; Zhang, Y.; Dong, W.K.; Ding, Y.J. A highly selective fluorescent chemosensor for CN⁻ a novel bis(salamo)-type tetraoxime ligand. *Spectrochim. Acta Part A* **2018**, *190*, 111–115. [[CrossRef](#)] [[PubMed](#)]
12. Dong, X.Y.; Li, X.Y.; Liu, L.Z.; Zhang, H.; Ding, Y.J.; Dong, W.K. Tri- and hexanuclear heterometallic Ni(II)–M(II) (M = Ca, Sr and Ba) bis(salamo)-type complexes: Synthesis, structure and fluorescence properties. *RSC Adv.* **2017**, *7*, 48394–48403. [[CrossRef](#)]
13. Wu, H.L.; Wang, C.P.; Wang, F.; Peng, H.P.; Zhang, H.; Bai, Y.C. A new manganese(III) complex from bis(5-methylsalicylaldehyde)-3-oxapentane-1,5-diamine: Synthesis, characterization, antioxidant activity and luminescence. *J. Chin. Chem. Soc.* **2015**, *62*, 1028–1034. [[CrossRef](#)]
14. Dong, W.K.; Ma, J.C.; Zhu, L.C.; Zhang, Y. Self-assembled zinc(II)-lanthanide(III) heteromultinuclear complexes constructed from 3-MeOsalamo ligand: Syntheses, structures and luminescent properties. *Cryst. Growth Des.* **2016**, *16*, 6903–6914. [[CrossRef](#)]
15. Song, X.Q.; Peng, Y.J.; Chen, G.Q.; Wang, X.R.; Liu, P.P.; Xu, W.Y. Substituted group-directed assembly of Zn(II) coordination complexes two new structural related pyrazolone Salen ligands: Syntheses, structures and fluorescence properties. *Inorg. Chim. Acta* **2015**, *427*, 13–21. [[CrossRef](#)]
16. Dong, W.K.; Zhang, F.; Li, N.; Xu, L.; Zhang, Y.; Zhang, J.; Zhu, L.C. Trinuclear cobalt(II) and zinc(II) salamo-type complexes: Syntheses, crystal structures, and fluorescent properties. *Zeitschrift für Anorganische und Allgemeine Chemie* **2016**, *642*, 532–538. [[CrossRef](#)]
17. Song, X.Q.; Cheng, G.Q.; Liu, Y.A. Enhanced Tb(III) luminescence by d¹⁰ transition metal coordination. *Inorg. Chim. Acta* **2016**, *450*, 386–394. [[CrossRef](#)]
18. Dong, W.K.; Ma, J.C.; Zhu, L.C.; Zhang, Y. Nine self-assembled nickel(II)–lanthanide(III) heterometallic complexes constructed from a Salamo-type bisoxime and bearing N- or O-donor auxiliary ligand: Syntheses, structures and magnetic properties. *New J. Chem.* **2016**, *40*, 6998–7010. [[CrossRef](#)]
19. Song, X.Q.; Liu, P.P.; Xiao, Z.R.; Li, X.; Liu, Y.A. Four polynuclear complexes a versatile salicylamide salen-like ligand: Synthesis, structural variations and magnetic properties. *Inorg. Chim. Acta* **2015**, *438*, 232–244. [[CrossRef](#)]
20. Dong, W.K.; Ma, J.C.; Dong, Y.J.; Zhu, L.C.; Zhang, Y. Di- and tetranuclear heterometallic 3d-4f cobalt(II)-lanthanide(III) complexes derived from a hexadentate bisoxime: Syntheses, structures and magnetic properties. *Polyhedron* **2016**, *115*, 228–235. [[CrossRef](#)]
21. Liu, P.P.; Wang, C.Y.; Zhang, M.; Song, X.Q. Pentanuclear sandwich-type Zn^{II}–Ln^{III} clusters a new Salen-like salicylamide ligand: Structure, near-infrared emission and magnetic properties. *Polyhedron* **2017**, *129*, 133–140. [[CrossRef](#)]
22. Wu, H.L.; Pan, G.L.; Wang, H.; Wang, X.L.; Bai, Y.C.; Zhang, Y.H. Study on synthesis, crystal structure, antioxidant and DNA-binding of mono-, di- and poly-nuclear lanthanides complexes with bis(*N*-salicylidene)-3-oxapentane-1,5-diamine. *J. Photochem. Photobiol. B Biol.* **2014**, *135*, 33–43. [[CrossRef](#)] [[PubMed](#)]

23. Dong, W.K.; Zhang, J.; Zhang, Y.; Li, N. Novel multinuclear transition metal(II) complexes an asymmetric Salamo-type ligand: Syntheses, structure characterizations and fluorescent properties. *Inorg. Chim. Acta* **2016**, *444*, 95–102. [[CrossRef](#)]
24. Dong, Y.J.; Li, X.L.; Zhang, Y.; Dong, W.K. A highly selective visual and fluorescent sensor for Pb^{2+} and Zn^{2+} and crystal structure of Cu^{2+} complex-on a novel single-armed Salamo-type bisoxime. *Supramol. Chem.* **2017**, *29*, 518–527. [[CrossRef](#)]
25. Sun, Y.X.; Xu, L.; Zhao, T.H.; Liu, S.H.; Liu, G.H.; Dong, X.T. Synthesis and crystal structure of a 3D supramolecular copper(II) complex with 1-(3-[(E)-3-bromo-5-chloro-2-hydroxybenzylidene]amino)phenyl ethanone oxime. *Synth. React. Inorg. Met.-Org. Nano-Met. Chem.* **2013**, *43*, 509–513. [[CrossRef](#)]
26. Dong, W.K.; Wang, Z.K.; Li, G.; Zhao, M.M.; Dong, X.Y.; Liu, S.H. Syntheses, crystal structures, and properties of a Salamo-type tetradentate chelating ligand and its pentacoordinated copper(II) complex. *Zeitschrift für Anorganische und Allgemeine Chemie* **2013**, *639*, 2263–2268. [[CrossRef](#)]
27. Akine, S.; Dong, W.K.; Nabeshima, T. Octanuclear zinc(II) and cobalt(II) clusters produced by cooperative tetrameric assembling of oxime chelate ligands. *Inorg. Chem.* **2006**, *454*, 677–684. [[CrossRef](#)] [[PubMed](#)]
28. Dong, W.K.; Zhang, X.Y.; Zhao, M.M.; Li, G.; Dong, X.Y. Syntheses and crystal structures of 5-Methoxy-6'-hydroxy-2,2'-[ethylenedioxybis(nitrilomethylidene)]diphenol and its tetranuclear zinc(II) complex. *Chin. J. Inorg. Chem.* **2014**, *30*, 710–716.
29. Akine, S.; Taniguchi, T.; Dong, W.K.; Masubuchi, S.; Nabeshima, T. Oxime-Based Salen-Type Tetradentate Ligands with High Stability against Imine Metathesis Reaction. *J. Org. Chem.* **2005**, *70*, 1704–1711. [[CrossRef](#)] [[PubMed](#)]
30. Dong, W.K.; Li, X.L.; Wang, L.; Zhang, Y.; Ding, Y.J. A new application of Salamo-type bisoximes: As a relay-sensor for $\text{Zn}^{2+}/\text{Cu}^{2+}$ and its novel complexes for successive sensing of H^+/OH^- . *Sens. Actuators B Chem.* **2016**, *229*, 370–378. [[CrossRef](#)]
31. Wang, L.; Ma, J.C.; Dong, W.K.; Zhu, L.C.; Zhang, Y. A novel Self-assembled nickel(II)–cerium(III) heterotetranuclear dimer constructed from N_2O_2 -type bisoxime and terephthalic acid: Synthesis, structure and photophysical properties. *Zeitschrift für Anorganische und Allgemeine Chemie* **2016**, *642*, 834–839. [[CrossRef](#)]
32. Dong, W.K.; Li, G.; Wang, Z.K.; Dong, X.Y. A novel trinuclear cobalt(II) complex derived from an asymmetric Salamo-type N_2O_3 bisoxime chelate ligand: Synthesis, structure and optical properties. *Spectrochim. Acta Part A* **2014**, *133*, 340–347. [[CrossRef](#)] [[PubMed](#)]
33. Akine, S.; Morita, Y.; Utsuno, F.; Nabeshima, T. Multiple folding structures mediated by metal coordination of acyclic multidentate ligand. *Inorg. Chem.* **2009**, *48*, 10670–10678. [[CrossRef](#)] [[PubMed](#)]
34. Wang, B.J.; Dong, W.K.; Zhang, Y.; Akogun, S.F. A novel relay-sensor for highly sensitive and selective detection of $\text{Zn}^{2+}/\text{Pic}^-$ and fluorescence on/off switch response of H^+/OH^- . *Sens. Actuators B Chem.* **2017**, *247*, 254–264. [[CrossRef](#)]
35. Dong, W.K.; Zhang, L.S.; Sun, Y.X.; Zhao, M.M.; Li, G.; Dong, X.Y. Synthesis, crystal structure and spectroscopic properties of a supramolecular zinc(II) complex with N_2O_2 coordination sphere. *Spectrochim. Acta Part A* **2014**, *121*, 324–329. [[CrossRef](#)] [[PubMed](#)]
36. Hao, J.; Li, L.H.; Zhang, J.T.; Akogun, S.F.; Wang, L.; Dong, W.K. Four homo- and hetero-bimetallic 3d/3d-2s complexes constructed from a naphthalenediol-based acyclic bis(salamo)-type tetraoxime ligand. *Polyhedron* **2017**, *134*, 1–10. [[CrossRef](#)]
37. Chen, L.; Dong, W.K.; Zhang, H.; Zhang, Y.; Sun, Y.X. Structural variation and luminescence properties of tri- and dinuclear Cu^{II} and Zn^{II} complexes constructed from a naphthalenediol-based bis(Salamo)-type ligand. *Cryst. Growth Des.* **2017**, *17*, 3636–3648. [[CrossRef](#)]
38. Dong, W.K.; Ma, J.C.; Dong, Y.J.; Zhao, L.; Zhu, L.C.; Sun, Y.X.; Zhang, Y. Two hetero-trinuclear $\text{Zn}(\text{II})\text{-M}(\text{II})$ ($\text{M} = \text{Sr}, \text{Ba}$) complexes metallohost of mononuclear $\text{Zn}(\text{II})$ complex: Syntheses, structures and fluorescence properties. *J. Coord. Chem.* **2016**, *69*, 3231–3241. [[CrossRef](#)]
39. Dong, Y.J.; Dong, X.Y.; Dong, W.K.; Zhang, Y.; Zhang, L.S. Three asymmetric Salamo-type copper(II) and cobalt(II) complexes: Syntheses, structures, fluorescent properties. *Polyhedron* **2017**, *123*, 305–315. [[CrossRef](#)]
40. Dong, Y.; Li, F.J.; Jiang, X.X.; Song, F.Y.; Cheng, Y.X.; Zhu, C.J. Na^+ triggered fluorescence sensors for Mg^{2+} detection a coumarin salen moiety. *Org. Lett.* **2011**, *9*, 2252–2255. [[CrossRef](#)] [[PubMed](#)]
41. Madison, W.I. *SAINT-Plus, Bruker Analytical X-ray System*; Bruker: Billerica, MA, USA, 1999.
42. Sheldrick, G.M. *SADABS, Program for Empirical Absorption Correction of Area Detector Data*; University of Gottingen: Gottingen, Germany, 1996.

43. Sheldrick, G.M. *SHELXS-97, Program for the Solution and the Refinement of Crystal Structures*; University of Gottingen: Gottingen, Germany, 1997.
44. Gao, L.; Wang, F.; Zhao, Q.; Zhang, Y.; Dong, W.K. Mononuclear Zn(II) and trinuclear Ni(II) complexes derived from a coumarin-containing N₂O₂ ligand: Syntheses, crystal structures and fluorescence properties. *Polyhedron* **2018**, *139*, 7–16. [[CrossRef](#)]
45. Dong, X.Y.; Akogun, S.F.; Zhou, W.M.; Dong, W.K. Tetranuclear Zn(II) complex an asymmetrical Salamo-type chelating ligand: Synthesis, structural characterization, and fluorescence property. *J. Chin. Chem. Soc.* **2017**, *64*, 412–419. [[CrossRef](#)]
46. Dong, W.K.; Lan, P.F.; Zhou, W.M.; Zhang, Y. Salamo-type trinuclear and tetranuclear cobalt(II) complexes a new asymmetry salamo-type ligand: Syntheses, crystal structures and fluorescence properties. *J. Coord. Chem.* **2016**, *65*, 1272–1283. [[CrossRef](#)]
47. Li, L.H.; Dong, W.K.; Zhang, Y.; Akogun, S.F.; Xu, L. Syntheses, structures and catecholase activities of homo-and hetero-trinuclear cobalt(II) complexes constructed from an acyclic naphthalenediol-based bis(salamo)-type ligand. *Appl. Organomet. Chem.* **2017**, *31*. [[CrossRef](#)]
48. Dong, W.K.; Akogun, S.F.; Zhang, Y.; Dong, X.Y. A reversible “turn-on” fluorescent sensor for selective detection of Zn²⁺. *Sens. Actuators B Chem.* **2017**, *238*, 723–734. [[CrossRef](#)]
49. Ma, J.C.; Dong, X.Y.; Dong, W.K.; Zhang, Y.; Zhu, L.C.; Zhang, J.T. An unexpected dinuclear Cu(II) complex with a bis(Salamo) chelating ligand: Synthesis, crystal structure, and photophysical properties. *J. Coord. Chem.* **2016**, *69*, 149–159. [[CrossRef](#)]
50. Zhang, Y.G.; Shi, Z.H.; Yang, L.Z.; Tang, X.L.; An, Y.Q.; Ju, Z.H.; Liu, W.S. A facile fluorescent probe coumarin-derived Schiff base for Al³⁺ in aqueous media. *Inorg. Chem. Commun.* **2014**, *39*, 86–89. [[CrossRef](#)]
51. Yang, L.; Powell, D.R.; House, R.P. Structural variation in copper(I) complexes with pyridylmethylamide ligands: Structural analysis with a new four-coordinate geometry index, τ_4 . *Dalton Trans.* **2007**, *9*, 955–964. [[CrossRef](#)] [[PubMed](#)]
52. Wu, H.L.; Bai, Y.C.; Zhang, Y.H.; Li, Z.; Wu, M.C.; Chen, C.Y.; Zhang, J.W. Synthesis, crystal structure, antioxidation and DNA-binding properties of a dinuclear copper(II) complex with bis(*N*-salicylidene)-3-oxapentane-1,5-diamine. *J. Coord. Chem.* **2014**, *67*, 3054–3066. [[CrossRef](#)]
53. Zheng, S.S.; Dong, W.K.; Zhang, Y.; Chen, L.; Dong, Y.G. Four Salamo-type 3d–4f hetero-bimetallic [Zn^{II}Ln^{III}] complexes: Syntheses, crystal structures, and luminescent and magnetic properties. *New J. Chem.* **2017**, *41*, 4966–4973. [[CrossRef](#)]
54. Chai, L.Q.; Huang, J.J.; Zhang, J.Y.; Li, Y.X. Two 1-D and 2-D cobalt(II) complexes: Synthesis, crystal structures, spectroscopic and electrochemical properties. *J. Coord. Chem.* **2015**, *68*, 1224–1237. [[CrossRef](#)]
55. Addison, A.W.; Rao, T.N.; Reedijk, J.; Rijn, J.V.; Verschoor, G.C. Synthesis, structure, and spectroscopic properties of copper(II) compounds containing nitrogen–sulphur donor ligands; the crystal and molecular structure of aqua[1,7-bis(*N*-methylbenzimidazol-2'-yl)-2,6-dithiaheptane]copper(II) perchlorate. *J. Chem. Soc. Dalton Trans.* **1984**, *7*, 1349–1356. [[CrossRef](#)]
56. Li, X.Y.; Chen, L.; Gao, L.; Zhang, Y.; Akogun, S.F.; Dong, W.K. Syntheses, crystal structures and catalytic activities of two solvent-induced homotrimeric Co(II) complexes with a naphthalenediol-based bis(Salamo)-type tetraoxime ligand. *RSC Adv.* **2017**, *7*, 35905–35916. [[CrossRef](#)]
57. Tao, C.H.; Ma, J.C.; Zhu, L.C.; Zhang, Y.; Dong, W.K. Heterobimetallic 3d–4f Zn(II)–Ln(III) (Ln = Sm, Eu, Tb and Dy) complexes with a N₂O₄ bisoxime chelate ligand and a simple auxiliary ligand Py: Syntheses, structures and luminescence properties. *Polyhedron* **2017**, *128*, 38–45. [[CrossRef](#)]
58. Wu, H.L.; Pan, G.L.; Bai, Y.C.; Wang, H.; Kong, J. Synthesis, structure, antioxidation, and DNA-binding studies of a binuclear ytterbium(III) complex with bis(*N*-salicylidene)-3-oxapentane-1,5-diamine. *Res. Chem. Intermed.* **2015**, *41*, 3375–3388. [[CrossRef](#)]
59. Dong, W.K.; Ma, J.C.; Zhu, L.C.; Zhang, Y.; Li, X.L. Four new nickel(II) complexes an asymmetric Salamo-type ligand: Synthesis, structure, solvent effect and electrochemical property. *Inorg. Chim. Acta* **2016**, *445*, 140–148. [[CrossRef](#)]
60. Liu, Y.A.; Wang, C.Y.; Zhang, M.; Song, X.Q. Structures and magnetic properties of cyclic heterometallic tetranuclear clusters. *Polyhedron* **2017**, *127*, 278–286. [[CrossRef](#)]
61. Liu, P.P.; Sheng, L.; Song, X.Q.; Xu, W.Y.; Liu, Y.A. Synthesis, structure and magnetic properties of a new one dimensional manganese coordination polymer constructed by a new asymmetrical ligand. *Inorg. Chim. Acta* **2015**, *434*, 252–257. [[CrossRef](#)]

62. Wang, L.; Li, X.Y.; Zhao, Q.; Li, L.H.; Dong, W.K. Fluorescence properties of heterotrinnuclear Zn(II)–M(II) (M = Ca, Sr and Ba) bis(salamo)-type complexes. *RSC Adv.* **2017**, *7*, 48730–48737. [[CrossRef](#)]
63. Zhang, H.; Dong, W.K.; Zhang, Y.; Akogun, S.F. Naphthalenediol-based bis(Salamo)-type homo- and heterotrinnuclear cobalt(II) complexes: Syntheses, structures and magnetic properties. *Polyhedron* **2017**, *133*, 279–293. [[CrossRef](#)]
64. Dong, X.Y.; Gao, L.; Wang, F.; Li, X.Y.; Zhang, Y.; Dong, W.K. Tri- and mono-nuclear zinc(II) complexes half- and mono-Salamo chelating ligands. *Crystals* **2017**, *7*, 267. [[CrossRef](#)]
65. Wang, L.; Hao, J.; Zhai, L.X.; Zhang, Y.; Dong, W.K. Synthesis, crystal structure, luminescence, electrochemical and antimicrobial properties of bis(salamo)-based co(II) complex. *Crystals* **2017**, *7*, 277. [[CrossRef](#)]
66. Chohan, Z.H.; Arif, M.; Sarfraz, M. Metal-based antibacterial and antifungal amino acid derived Schiff bases: Their synthesis, characterization and in vitro biological activity. *Appl. Organomet. Chem.* **2007**, *21*, 294–302. [[CrossRef](#)]



© 2018 by the authors. Licensee MDPI, Basel, Switzerland. This article is an open access article distributed under the terms and conditions of the Creative Commons Attribution (CC BY) license (<http://creativecommons.org/licenses/by/4.0/>).